International Journal of Multidisciplinary Approach and Studies

ISSN NO:: 2348 – 537X

Phonon Anomalies In Hfn And Zrn

Dr. Poonam Mishra,

Assistant Professor, Department of Physics,

Government Kaktiya P. G. College Jagdalpur, Chhattisgarh

ABSTRACT:

The phonon dispersion curve are determined by model (BSM) for the crystals transition metal mono-nitrides (HfN and ZrN) and compared with the experimental phonons, which forms perhaps the best test for this purpose. The eight numbers of parameters of the model are determined by using the some set of input data. The results and degrees of agreement obtained in each case show clearly the superiority of the "charge-transfer mechanism" for representing the deformations of electron shells used in the BSM. The phonon dispersion curves and phonon density of states in HfN and ZrN have been measured in high-symmetry directions Δ, Σ and Λ by breathing shell model (BSM). Anomalies in the dispersion of the acoustic branches and optical branches have been detected which are well described by experimental results.

***Keywords**: Lattice dynamics, phonons in crystal lattices, thermal properties of crystalline solids, phonon states and phonon dispersion*

PACS no: 63, 63.20.-e, 65.40.-b, 63.20. Dj.

1. INTRODUCTION

Besides a number of exciting physical properties, transition metal (TM) nitrides compounds adopt several crystal structures. It is well known that TMN can crystallize in different crystal lattices and form different phases depending on the R_x/R_M ratio where R_M and R_x are the atomic radii of metallic and non-metallic atoms, respectively. Almost all the nitrides of transition metals with the MX stoichiometry are usually cubic, where the metallic atoms form

the face-centered cubic (fcc) sublattice and non-metallic atoms occupy interstitial positions, forming NaCl-type structure and for many of them, the phonon dispersion curves have been measured by coherent inelastic neutron scattering [1-10]. The phonon dispersion curves reflect the extreme hardness and high melting points by the steep slopes of the acoustic branches in the long-wavelength range and by the relatively high-lying optic branches, separated from the acoustic part of the spectrum by a frequency gap of a few terahertz. The general nature of the optic branches is for most of the transition-metal nitrides, similar to that of ionic compounds with the rock-salt structure. The longitudinal branches (LO) lie above the transverse branches (TO), due to the long-range Coulomb interactions that are screened by the conduction electrons. This metallic screening destroys the Lyddane-Sachs-Teller Splitting [11] and results in a degeneracy of the LO and TO modes at the center of the Brillouin zone. However for most of the transition-metal compounds the screening vector is small compared to the dimensions of the Brillouin zone. The LO branches therefore recover quickly from the screening effect and are for most of the transition-metal nitrides found above the TO branches. The only exceptions are UC [3], UN [5] and as the results of the present measurements show HfN, ZrN.

The most successful model so far in reproducing the measured phonon dispersion curves of transition metal carbides and nitrides with rocksalt structure in the breathing shell model [15]. We shall use breathing shell model (BSM) for the purpose of assessing the role played by the breathing motion of the valance electrons, introduced in this model phenomenologically. Here we will use a breathing shell model theory to calculate complete phonon dispersion curves, phonon density of states and specific heat for transition metal mononitride (HfN and ZrN) compounds. In addition, the effect of anion and cation polarizabilities on the phonon spectrum can also be analysed by this theory. The anomalies in the dispersion of the acoustic branches and optical branches have been detected which are well described by experimental results.

2. THEORY OF MODEL APPLIED

The Breathing Shell Model (BSM) is used in these two transition metal mono-nitride compounds HfN and ZrN to interpret the phonon anomalies of calculated results with the experimental results. In this model [15] the isotropic deformation of spherical electron shells is considered in the form of expansion and /or contraction of these shells during lattice

vibrations. This 'breathing' is considered as an extra degree of freedom, and the 'adiabatic approximation' is obeyed by associating zero kinetic energy with it. Using the shell model notations of woods et.al. [17] and introducing these ideas in the theory of SM, we get the basic equations of motion for BSM as follows:

$$\mathbf{D(q)=(R'+ZCZ)-(R'-ZCY)(R'+G+YCY)^{-1}(R'+YCZ)} \quad (1)$$

where R'= $(R-QH^{-1}Q^{\dagger})$; C and R are the Coulomb and short-range repulsive interaction matrices respectively. Q is (6×2) matrix representing the interactions between the ion displacements and breathing mode variables. The H is a (2×2) matrix and represents the interactions between the breathing mode variables of different ions in the lattice. These breathing matrices Q and H are written as [15]

$$Q = \begin{bmatrix} 0 & D \\ D & 0 \end{bmatrix} \quad (2)$$

D is a 3-vector breathing matrix. The explicit expressions for these dynamical matrix is as follows:

$$D = -iA \begin{bmatrix} \sin q_\alpha r_o \\ \sin q_\beta r_o \\ \sin q_\gamma r_o \end{bmatrix} \quad (3)$$

with

$$H = \begin{vmatrix} H(11) & H(12) \\ H(21) & H(22) \end{vmatrix} \quad (4)$$

H(11)== $3A+G_1$, H(22)= $3A+G_2$, and

$$H(12)=H(21)=A\left(\cos q_\alpha r_o + \cos q_\beta r_o + \cos q_\gamma r_o\right) \quad (5)$$

G and A are the diagonal matrices and represent the core-shell interaction and shell charge, respectively. The G_1 and G_2 can be expressed as

$$\frac{\partial^2 V_{CS}^{(1)}}{\partial r^2} = \frac{e^2}{V} G_1 \quad (6)$$

$$\frac{\partial^2 V_{CS}^{(2)}}{\partial r^2} = \frac{e^2}{V} G_2 \qquad (7)$$

where $V_{CS}^{(1)}$ and $V_{CS}^{(2)}$ are the core shell interaction potentials for ion number 1 and 2 respectively. The parameter involved in the dynamical matrix ***D(q)*** are determined by their relation with some microscopic experimental data, i.e. elastic constant, dielectric constant and zone center phonon frequencies. In order to minimize the number of parameters, we have assumed the shell charges, $Y_1=Y_2=Y$. The parameters are tabulated in the Tables.

3. RESULTS AND DISCUSSION

The phonon spectra obtained above have been used to predict the phonon dispersion relations $w_j(q)$ which are measured from inelastic neutron scattering. We will also bring out detailed discussion on the force constants various charge parameters and the role of ionic polarizabilities on phonon spectrum in these two (HfN and ZrN) compounds. We first calculated the phonon dispersion curves for two TMN systems HfN and ZrN by using breathing shell model (BSM), which has been used by jha and co worker [12-14] to explain satisfactorily the anomalous phonon properties in rare earth chalcogenides and pnictides. Followed by this we will present the one-phonon density of states and specific heat, which provide the most dependable test of any model.

(i) Phonon dispersion relations. The phonon dispersion relations along principal symmetry directions Δ, Σ and Λ, using a phenomenological model theory, which include the short-range breathing motion of the valance electrons. The results obtained from the breathing shell model [15] have also been displayed in these visual comparison.

For this purpose we derive the model parameters self consistently, using known macroscopic properties. These properties include equilibrium lattice constant, elastic constants, zone center vibrational frequencies, ionic polarizabilities and dielectric constants. The input data used for this purpose are given in Table1. and also output parameters are listed in Table2.

The phonon dispersion curves (PDC) of HfN and ZrN have been displayed in Figs.1-2 and compared them with their neutron data [8, 16]. The measured data from (BSM) model are compared to the results of experimental inelastic neutron scattering values. ○ and ▲ represents the experimental points of longitudinal and transverse phonons respectively. The

simple nature of the optic branches is for most of the transition metal carbides and nitrides, similar to that of ionic compounds with the rock-salt structure. The longitudinal branches (LO) lie above the transverse branches (TO) due to the long-range coulomb interactions that are screened by the conduction electrons. In optic and acoustic branches are separated by an energy gap. It is revealed from Fig.1 and 2. that in case of HfN and ZrN the theoretical results of PDC are in very good agreement with experimental data along (q 0 0), (q q 0) and (q q q) directions for LO, TO and LA, TA modes. Because of the screening due to conduction electrons the LO and TO modes are degenerate at the **Γ** point, whereas the splitting of LO and TO modes at the **L** point is due to the long-range coulomb interaction which is not completely screened at larger **q** vectors. Strong electron-phonon interactions might be responsible for such peculiar behaviours

(ii) One-Phonon density of nitride compounds: In Figs 3 and 4, we have plotted one phonon density of states of HfN and ZrN and compare it with neutron scattering measurement (experimental) [8]. Our calculated results agree satisfactorily with the neutron scattering data. Our prediction of a peak at about 15.1THz (Fig. 1.) due to optical phonon at X-point in HfN is in accordance with experimental observation [16]. The peaks observed at 50.04 cm^{-1}, 83.4 cm^{-1}, 133.44 cm^{-1} and 200.16 cm^{-1} are longitudinal and transverse acoustical phonons, while the longitudinal and transverse optical peaks are observed at 467.04 cm^{-1}, 500.4 cm^{-1} and 567.12 cm^{-1} respectively. A peak at about 14.90 THz due to optical phonon at X-point in ZrN (Fig. 2.) is in accordance with experimental observation [8]. In ZrN peaks are observed at 66.72 cm^{-1}, 100.08 cm^{-1}, 166.8 cm^{-1} and 200.16 cm^{-1} from our BSM model and neutron inelastic scattering results are observed at 178 and 230 cm^{-1} for LA and TA branches respectively. For LO and TO branch peaks are observed at 433.68 cm^{-1}, 483.72 cm^{-1} and 583.8 cm^{-1} from BSM model and neutron result is observed at 497 cm^{-1} respectively. From these results we conclude that the calculated values from BSM model are in good agreement with the experimental datas [8].

(iii) *Specific heat of nitride compounds:* Einstein took the atoms of a crystal to be independent oscillators each having the same (circular) frequency ω_E and able to vibrate freely in space. The energy of each oscillator was quantized in units of $\hbar\omega_E$, and showed that the average energy of a crystal of N atoms at temperature T would then be given by

$\bar{U}$= 3Nħ ω_E/exp(ħ ω_E/k_BT)-1

where K_B is Boltzmann's constant. The specific heat is then given by

$C_v = \frac{\overline{dU}}{dT}$ C_v is shown as a function of T/θ_E, where θ_E is a convenient abbreviation for $\hbar\omega_E/k_B$ and has the dimensions of temperature. C_v is zero at T=0 and rises asymptotically to the value $3Nk_B = 3R$ when T» θ_E. For high temperatures therefore, quantization is unimportant and the specific heat has the same value as if each degree of freedom of the system had energy $\frac{1}{2}k_BT$, where as at lower temperatures there is a pronounced deviation from this result of the theorem of energy.

Theoretical results for the lattice specific heat, obtained from phonon densities calculated on the basis of appropriate shell model (BSM). In Figs 5 and 6, we have also reported the

Input Parameters	HfN	ZrN

calculated value of specific heat at constant volume as a function of temperature for the first time. In the inset we have presented the variation of specific heat up to 100K. These features are the same as are expected in a simple NaCl structure compounds.

ACKNOWLEDGEMENT

The author PM is thankful to University Grant Commission (U.G.C), New Delhi India for the award of Junior Research Fellow [UGC project no. F.31-4/2005 (SR)] for financial support to this work. MA is thankful to MPCST for financial support.

Table 1. Input Parameters of Transition metal mono-nitrides

$\mathbf{a_0}$ (Å)	4.52	4.72
$\mathbf{C_{11}}$ (Mbar)	5.66	3.98
$\mathbf{C_{12}}$ (Mbar)	1.39	0.98
$\mathbf{C_{44}}$ (Mbar)	1.39	0.98
ν_{TO} (Γ) THz	14.99	14.38
$\varepsilon_0 = \varepsilon_\infty$	3.60	2.69
α_1 (Å^3)	0.162	0.179
α_2 (Å^3)	1.10	1.10

Table 2. Model Parameters for Transition compounds using BSM. All are in units of $e^2/2V$ except Y in units of e.

Input Parameters	HfN	ZrN
A_{12}	55.28	33.32
B_{12}	-1.17	1.03
A_{11}	30.46	25.21
B_{11}	-9.99	-7.28
B_{22}	-17.86	-12.37
Z	1.68	1.00
$Y=Y_1=Y_2$	-2.78	-2.35
G_1	2.26	816.75
G_2	1104.10	41.96

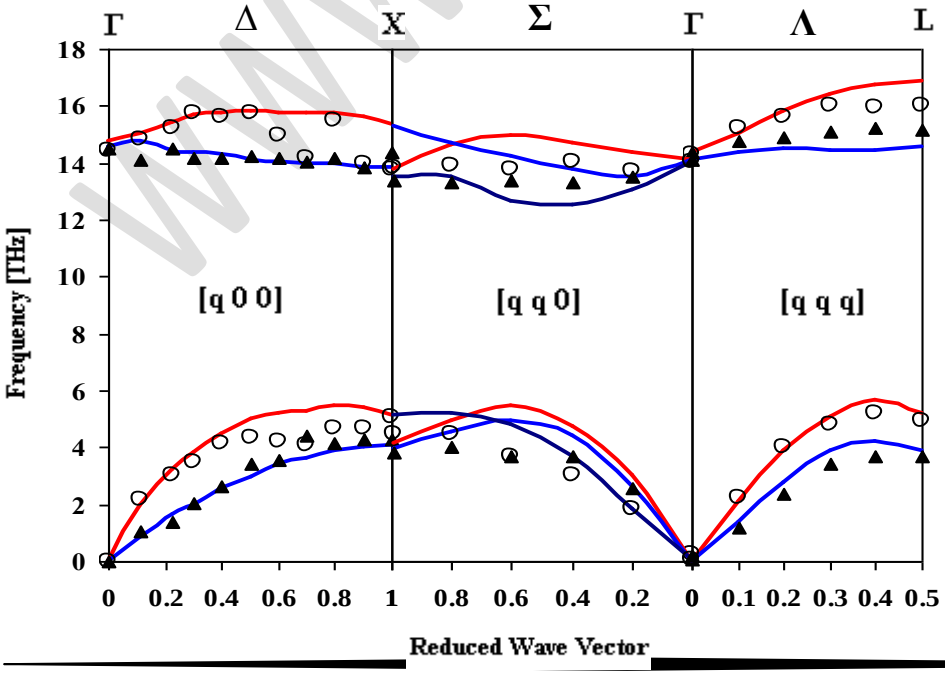

International Journal of Multidisciplinary Approach and Studies
ISSN NO:: 2348 – 537X

Fig 1. Phonon dispersion curve for HfN, red and blue, black lines, are longitudinal and transverse phonons were calculated from BSM fit; ○ and ▲ shows experimental points of longitudinal and transverse phonons respectively.

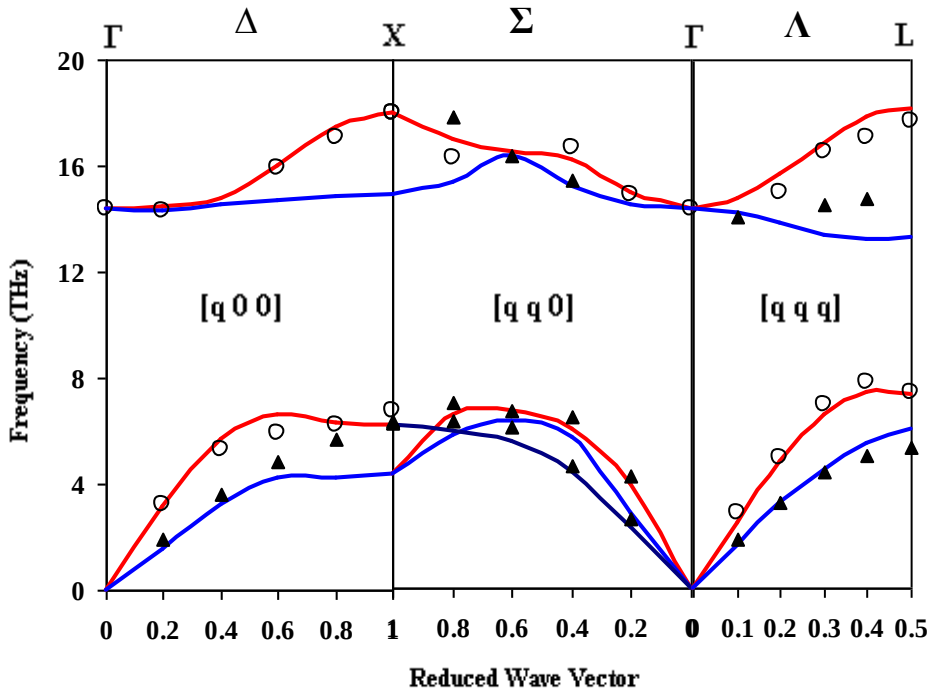

Fig 2. Phonon dispersion curve for ZrN, red and blue, black lines, are longitudinal and transverse phonons were calculated from BSM fit; ○ and ▲ shows experimental points of longitudinal and transverse phonons respectively.

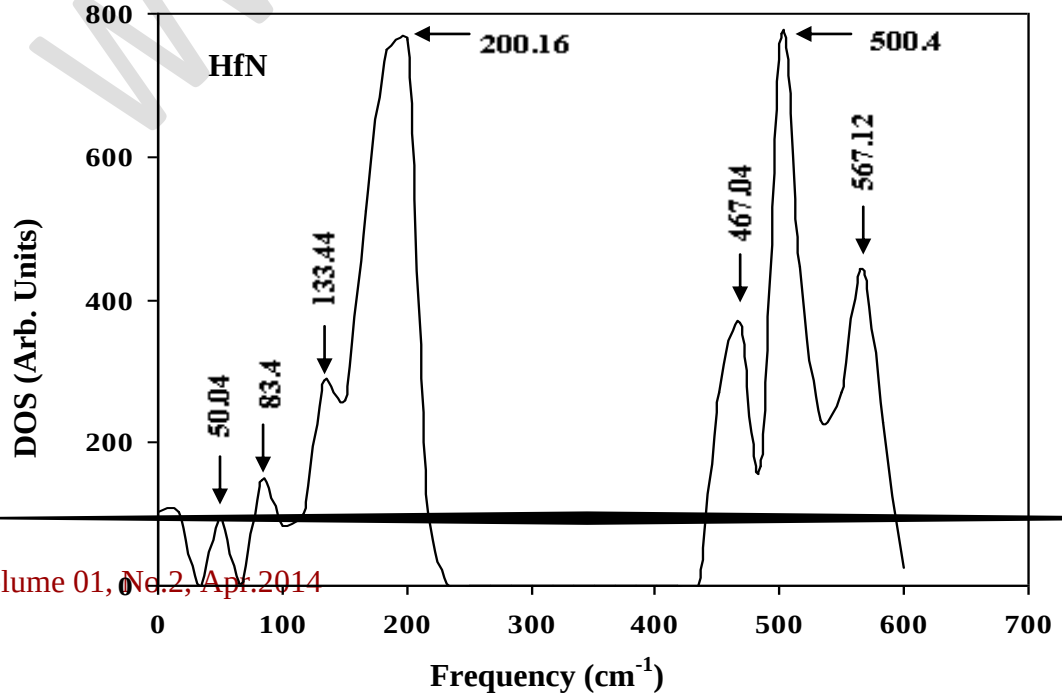

Fig 3. One-Phonon density of States of HfN calculated from BSM

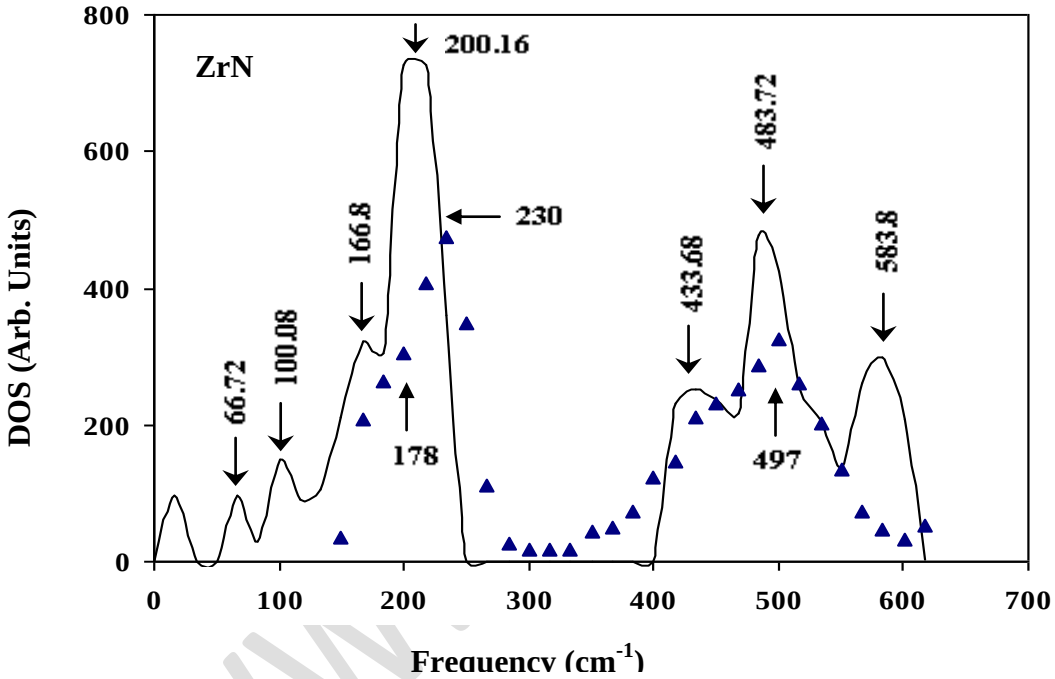

Fig 4. One-Phonon density of States of ZrN calculated from BSM

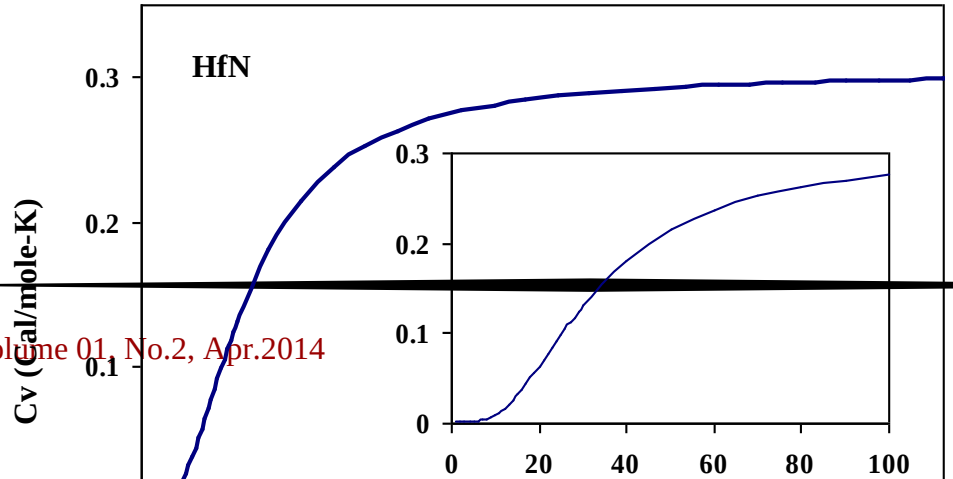

Fig 5. Specific heat of HfN at constant volume as a function of temperature

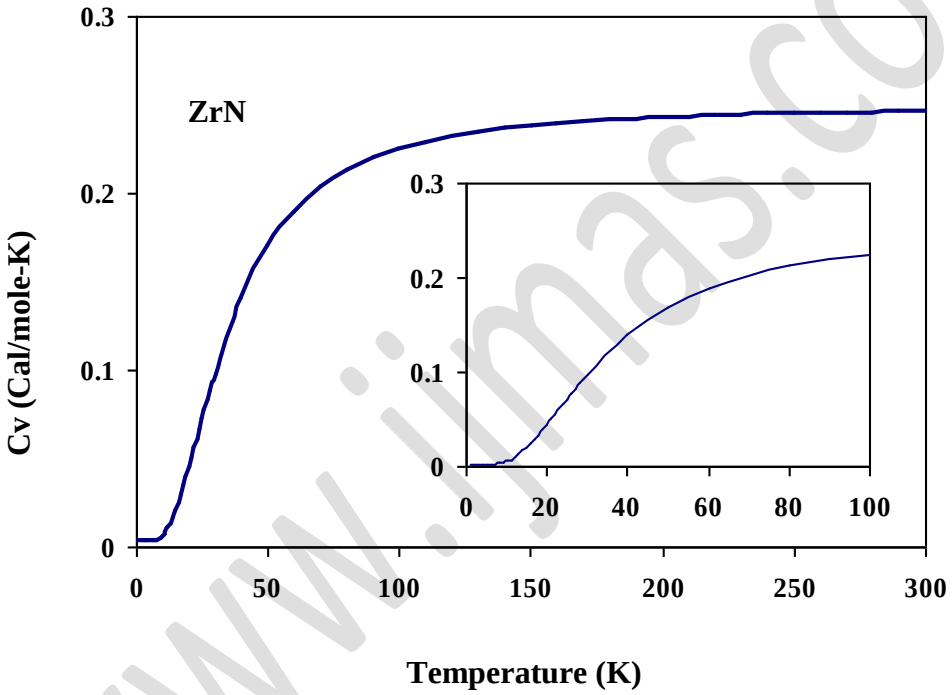

Fig 6. Specific heat of ZrN at constant volume as a function of temperature

REFRENCES

1. H G Smith and W Gläser, Phys. Rev. Lett. **25**, 1611 (1970)
2. H G Smith and W Gläser, in Phonons, edited by M A Nusimovisci (Flammarion, Paris) p. 145 (1971)

3. H G Smith, in Superconductivity in d- and f-Band Transition Metals (Rochester), Proceedings of the Conference on Superconductivity in d- and f-Band Metals, edited by D H Douglas (AIP, New York), p. 321 (1972)
4. L Pintschovius, W Reichardt, and B Scheerer, KFK Report No. 2538, (unpublished) p. 4 (1977)
5. G Dolling, T M Holden, F C Svensson, W J T Ruyers, and G H Lander, in Lattice Dynamics, edited by M Balkanski (Flammarion, Paris, 1978), p. 81
6. L Pintschovius, W Reichardt, and B Scheerer, *J. Phys. C* **11**, 1557 (1978)
7. W Kress, P Roedhammer, H Bilz, W D Teuchert and A N Christensen, *Phys. Rev.* **B 17**, 111 (1978)
8. A N Christensen, O W Dietrich, W Kress, and W D Teuchert, *Phys. Rev. B* **19**, 5699 (1979)
9. W Weber, P Roedhammer, L Pintschovius, W Reichardt, F Gompf, and A N Christensen, *Phys. Rev. Lett*. **43**, 868 (1979)
10. A N Christensen, O W Dietrich, W Kress, W D Teuchert, and R Currat, *Solid State Commun.* **31**, 795 (1979)
11. R H Lyddane, R G Sachs, and E Teller, *Phys. Rev.* **59**, 673 (1941)
12. P K Jha, S P Sanyal, *Phys. Rev.* **B 46**, 3664 (1992)
13. P K Jha, S P Sanyal, *Physica* **B 216,** 125 (1995)
14. M Aynyas, P K Jha, S P Sanyal, *Ind. J. Pure and Appl. Phys.* **43**, 109 (2005)
15. R K Singh, *Phys. Reports* **85**, 259 (1982)
16. A N Christensen, W Kress, M Miura, and N Lehner, *Phys. Rev.* **B 28,** 977 (1983)
17. A D B Woods, W Cochran and B N Brockhouse, *Phys. Rev.* 119, 980-99 (1960)